ELSEVIER

Ceramics International 30 (2004) 2157–2162

CERAMICS INTERNATIONAL

www.elsevier.com/locate/ceramint

The superplastic deep drawing of a fine-grained alumina–zirconia ceramic composite and its cavitation behavior

Guoqing Chen*, Kaifeng Zhang, Guofeng Wang, Wenbo Han

School of Materials Science and Engineering, Harbin Institute of Technology, Harbin 150001, PR China

Received 5 September 2003; received in revised form 2 November 2003; accepted 9 December 2003
Available online 9 April 2004

Abstract

The synthesis, superplastic deep drawing and cavitation behavior of a fine-grained alumina–zirconia ceramic composite have been investigated. The results show that dense Al_2O_3/ZrO_2 samples with average grain diameter of 230 nm can be elongated to a dome height of at least 12 mm at the punch rate of 0.6 mm·min^{-1} at 1400 °C. Deformed microstructure of the material indicates that not only the nucleation and growth of internal cavities are effectively suppressed but also the intragranular dislocation structures and sub-boundaries are observed around the nano-particles in alumina grains, which proves that intragranular dislocation creep is playing an important role in deformation. While the research on the deep drawing of the materials with the initial average grain size of 450 nm conforms that a plasticity controlled cavity growth process takes place during deformation.

Keywords: B. Composites; C. Plasticity; D. Al_2O_3; D. ZrO_2; Cavitation

1. Introduction

Cavitation during superplastic deformation is of practical concern, not only because it affects the optimum elongation but also because of the deterioration in the subsequent room-temperature properties. Experimental results indicate that even small level of cavitation may sometimes lead to a dramatic degradation in mechanical properties [1]. The factors influencing cavity nucleation during superplastic flow include those relating to microstructure such as grain boundary particles, grain size, phases and those associated with deformation conditions such as strain, strain rate, stress and temperature.

Some fundamental information on the characteristics of cavity development in uniaxial tension has been obtained [2–4]. However, in industrial forming the strain condition is always biaxial deformation or plane strain state. In order to reduce cavitation level, it is important to understand the microstructure and deformation parameters that affect the cavitation behavior under multi-axial deformation. In the present paper biaxial tension (deep drawing) results are described on Al_2O_3–ZrO_2 ceramics with varying grain sizes. The influence of experimental conditions (punch displacement rate and operation temperature) on deep drawing is examined. Focus has been placed on the evolution of cavitation during biaxial tension at strain rates higher than those available for Al_2O_3-based materials examined in earlier studies [4–7]. On examination of cavitation behavior and deformed microstructures, we discuss the role of second phase dispersion in the superplasticity and relating mechanisms of the present material.

2. Materials and experimental procedures

Nano-sized Al_2O_3–20 mol%ZrO_2(3Y) (20 mol%ZrO_2 = 16.9 vol.%ZrO_2 = 23.6 wt.%ZrO_2) powders were synthesized by heating of ethanol-aqueous salt solutions combined with co-precipitation method [8]. The Al_2O_3–ZrO_2 ceramic materials were made from two different types of powder with different agglomerations. One powder was synthesized by using ammonia as precipitant, where the agglomerates are hard. This final powder typically has a BET surface area of 51 m^2·g^{-1}. The second powder with a BET surface area of 69.5 m^2·g^{-1} was prepared using ammonium hydrogen carbonate as a precipitant, where the powder was loosely

* Corresponding author. Tel.: +86-451-86413942; fax: +86-451-86418763.gqchen@hit.edu.cn

0272-8842/$30.00
doi:10.1016/j.ceramint.2003.12.002

Table 1
The samples used for deformation tests by deep drawing

Code	Sintering temperature (°C)	Holding time (h)	d_A (nm)	d_Z (nm)	Average grain size (nm)	Relative density (%)
A[1]	1450	1	280	120	230	96.2
B[1]	1550	1	480	160	450	
C[2]	1450	2	550	210	490	97.0
D[2]	1550	2	900	370	870	99.1

[1] Represents the soft agglomerated powder which was precipitated using ammonium hydrogen carbonate.
[2] Represents the hard agglomerated powder which was precipitated using ammonia.
d_A: average grain diameter of the alumina phase; d_Z: average grain diameter of the zirconia phase.

agglomerated. The effect of the precipitant on agglomeration was studied in ref. [9]. An X-ray diffraction study revealed that a minimum temperature of 1100 °C is required to convert the ($\delta + \gamma$)-Al_2O_3 to hexagonal α-corundum phase. The two types of powder were calcined at 1100 °C to obtain a nanocrystalline powder. The average crystallite size of 20–25 nm was calculated from TEM photographs of two powders. The theoretical density of the final corundum +20 mol%YTZ product is 4.315 g·cm^{-3}. Ceramic composites were made from each powder. The as-obtained powders were uniaxially pressed at 10 MPa in a cylindrical die with diameter of 30 mm at room temperature, and subsequently hot pressing sintering was conducted in vacuum at 50 MPa in the same die to produce sintered compacts.

Deformation by means of deep drawing was performed on four different Al_2O_3–ZrO_2 composites, coded A, B, C and D. More details of the materials used for deformation are given in Table 1. Grain sizes were determined from SEM micrograph using the linear intercept method for the polished and thermally etched samples. The average grain sizes of the two-phase material were determined as 1.56 times the average linear intercept length of grains. Deep drawing tests were performed on several discs of each material. All discs were machined to a diameter of 30 mm and a thickness of 1 mm. The discs were placed on a cylindrical SiC ring with an inner diameter of 22.5 mm. A hemispherical punch with radius of 9 mm was pushed on one side of the ceramic using different velocities (0.2–1.0 mm·min^{-1}), and the force was monitored at the same time. The tests were performed in vacuum at 1350, 1400 and 1450 °C using High-multi 10 000 testing machine (USA). The axial displacement was measured externally during all tests. Microstructure examination of specimens was carried out at the center of the as-polished portion using scanning electron microscope (SEM, Philips XL 20) equipped with an image analyzer. Quantitative measurements of cavities were performed on the cavitated area fraction, which corresponds to the cavity volume fraction. For cavities characterization, specimens were mechanically polished to 1 μm diamond finish and the surfaces quantitatively examined using optical microscope connected to an image analysis system (Magiscan) with software capable of counting and sizing discrete cavities by automatically scanning any selected region of the image. Philips CM12 transmission electron microscope was used to examine the deformed microstructure of samples.

The results in Table 1 show that very fine-grained and dense Al_2O_3–ZrO_2 with average grain size of 230 nm can be obtained, when starting with powder A[1]. By using different powders and sintering procedures different grain sizes were obtained in final ceramics. Using this set of samples the influence of grain size on deformation behavior can be analyzed.

3. Results and discussions

3.1. Influence of grain size on deep drawing

For largely enhanced tensile ductility in alumina-based ceramics the following considerations are necessary. One is the reduction of grain size, which is a widely accepted prerequisite for superplasticity. The other concerns the density of residual defects and homogeneity of particle dispersion when a second phase coexists. The microstructure of our ceramic material shows a two-phase microstructure consisting of equiaxed alumina grains and small zirconia particles dispersed at the multiple grain junctions (Fig. 1). The as-sintered material is a typical intragranular/intergranular nanocomposite (see TEM picture, Fig. 7a). The average grain size of 230 nm is 40% or more smaller than those of materials prepared by conventional processing [3,7,10,11].

The grain-size effect on superplasticity has been often observed in literature and can be explained by the fact that

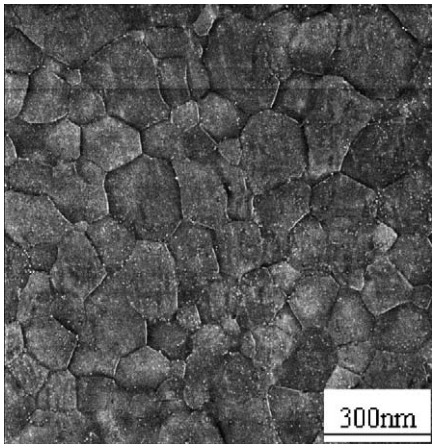

Fig. 1. The microstructure of as-sintered composite.

grain boundary sliding is the dominant deformation mode. High-temperature deformation behavior in fine-grained ceramics is often described by:

$$\dot{\varepsilon} = A\frac{\sigma^n}{d^p}\exp\left(-\frac{Q}{RT}\right) \quad (1)$$

where $\dot{\varepsilon}$ is the strain rate, σ is the flow stress, d is the grain size, Q is the apparent activation energy, R is the gas constant, T is the absolute temperature, A is a proportionality constant, and n and p are the stress and grain size exponents, respectively. Generally, superplastic deformation occurs in ceramics due to grain boundary sliding. Accompanying the grain boundary sliding the general understanding is that accommodation involving diffusion and/or dislocation movement is required to maintain grain boundary cohesion. If accommodation is incomplete or slower than the grain displacement rate then cavities will occur. The effect of grain growth or size is to make the accommodation process more difficult by increasing the unit path length for the operative mechanism. In other words, reducing the grain size still gives sufficient high strain rates at lower temperature. It is shown in Fig. 2 that at a relatively high punch rate of 0.6 mm·min^{-1} the composite with the average grain size of 230 nm (sample A^1) could be deep-drawn at 1400 °C to a height of 12 mm (maximum stroke of the die) without fracture while the coarser-grained samples D^2 and B^1 fractured after punch displacements of 8 and 10.7 mm, respectively. Fracturing is indicated in Fig. 3 by an arrow downwards. When the punch rate is 0.6 mm·min^{-1}, the mean maximum strain rate in deformation is higher than 1.0×10^{-3} s^{-1}, which is higher than those in previous uniaxial tensile tests in alumina-based ceramics [4–7]. With the initial average grain size of 230 nm superplastically formed net-shaped articles from alumina–zirconia ceramic sheets are limited only by the die design (Fig. 4). The ceramic can behave this way because the original materials create a mix of two types

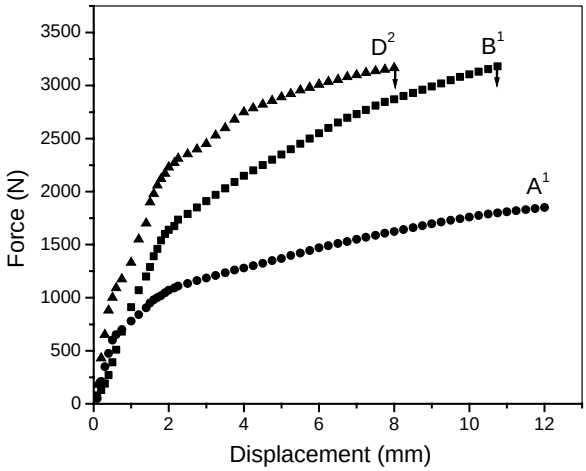

Fig. 2. Displacement vs. applied force during deep drawing at 1400 °C of several ceramics with different grain sizes (A^1: 230 nm, B^1: 450 nm, D^2: 870 nm; see Table 1). Displacement rate: 0.6 mm·min^{-1}.

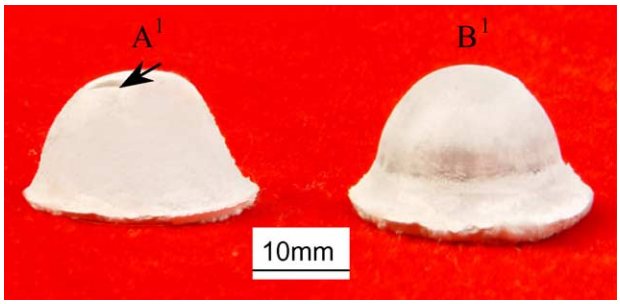

Fig. 3. Sample A^1 (230 nm) and B^1 (450 nm) after deformation tests as given for Fig. 2 (the arrow indicating the fracture).

of grain that suppresses the growth of individual grains, and small particle size permits the material to easily stretch. At the same time the cavity generation and growth is effectively suppressed.

The increased deformability to failure with decreasing grain size is probably a consequence of increased grain boundary sliding in the fine-grained materials and a result of decreased local stresses; in coarser grained materials, these stresses enhance cavitations propagation, thereby limiting the high temperature ductility. The reduction in grain size, therefore, does not result in a noticeable change in strain hardening rate, but it does lead to a persistent reduction in flow stress by about 20 MPa and extend the hardening regions. Fig. 2 also shows that with increasing grain size, the slope of the curves also increases. This demonstrates that strain hardening increases when grain size increases, which is consistent with the conclusion deduced by comparing the tensile flow stress for the two different grain sizes of 450 and 1000 nm in this material in ref. [5].

3.2. Punch rate and deformation temperature

It is obvious from the results in Fig. 5 that the experimental conditions (temperature and punch rate) influence deformation. By increasing the punch rate the maximum elongation decreases while a higher force is necessary for obtaining the same displacement. The relation between

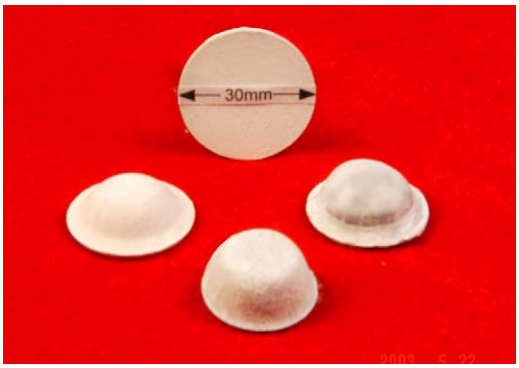

Fig. 4. Net-shaped articles superplastically formed from alumina-based ceramic sheet with the average grain size of 230 nm are limited only by the die design.

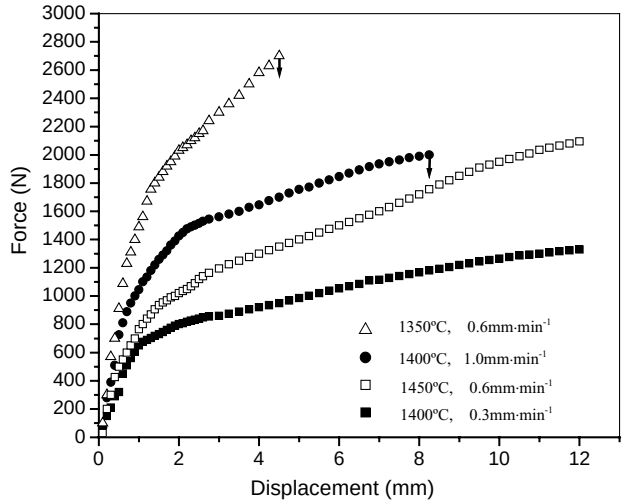

Fig. 5. Displacement vs. applied force during deep drawing at different deformation conditions with the average grain size of 230 nm.

punch rate and force, necessary for a certain displacement, will now be discussed in terms of the phenomenological law as given by Eq. (1). At 1400 °C a force of 1625 N (F_1) is necessary for obtaining a displacement of 8 mm at a punch rate of 0.6 mm·min^{-1} (coded as v_1), while the same displacement is achieved at a punch rate of 0.3 mm·min^{-1} by using a force of about 1170 N (F_2) on an identical surface area (coded as v_2; Fig. 5). The ratio of the stresses applied on samples A^1 and A^2 is identical to the ratio of the forces (F_1/F_2). The ratio of strain rates is identical to the ratio of the punch rates (v_1/v_2). In this way a relation between the ratios of strain rates and stresses for samples with identical grain size can be written as follows [12]:

$$\frac{v_1}{v_2} = \left(\frac{F_1}{F_2}\right)^n \tag{2}$$

From this equation a stress exponent (n) of 2.1 has been calculated, using the above mentioned data. This value has been confirmed by comparing several force ratios at different displacements for the samples. The n-value for the present material is nearly consistent with those for the Al_2O_3–10 vol.%ZrO_2 ($n = 2.4$) [5] and Al_2O_3–10%ZrO_2–10%MgO·1.3Al_2O_3 ($n = 2.2$) [7]. It is difficult to calculate the stress on the samples under these experimental conditions, but it is assumed that a maximum stress of 25 MPa is imposed on a sample when applying a load of 1700 N, which is the load used at punch rate of 0.6 mm·min^{-1} at 1400 °C for forming a hemisphere with a radius of 9 mm (see Fig. 2).

This influence of punch rate and deformation temperature on deformation can be explained in terms of cavity formation during tensile deformation [12]. It is widely accepted that cavity nucleation arises from stress concentrations generated at second phase particles or triple points as a result of grain boundary sliding. At a certain concentration and/or size the cavities are interlinking which is associated with the onset of tensile failure. Because of the stronger cavity growth at higher strain rate also higher stresses are present in the ceramics. This explains the higher forces necessary for the same displacement at higher punch rates. Fig. 5 also indicates that under a constant strain rate the degree of cavitations increases with a decrease in deformation temperature.

3.3. Cavitation behavior in deep drawing and deformed microstructure

Cavity nucleation is a very complex problem since cavities can either nucleate or possibly develop from pre-existing cavities. In the present study, the deformability of the samples with different grain sizes was quite different (Fig. 2). A comparison of the deformed microstructure with varying initial grain sizes (230 and 450 nm) threw light on the difference of their deformability. Fig. 6 shows the cavity morphology of the samples with the initial grain size of 450 nm during deformation. It can be seen that in early stage cavities nucleate mainly at grain boundary particles or at triple points and grow toward the matrix grain size. Most of the cavities are crack-like voids (Fig. 6a). Fig. 6b shows a typical cavity size distribution in deep drawing. With the increasing of the deformation the cavities extended and linked up rapidly, thus developed into strip voids distributed homogeneously to every direction (Fig. 6b). Fig. 6c shows that cavities can become considerably larger than the average grain size with areas up to several square microns. Earlier studies [2–4] have shown that concurrent cavitation, in particular cavity interlinkage in the direction normal to the stress axis limits the tensile ductility of superplastic ceramics. Also they have demonstrated that the fine cavities do not grow readily to the large ones because cavity growth exceeding the current grain size is constrained by the surrounding matrix [4]. In the present material, however, a different feature was observed in the biaxial tensile deformation. Cavity growth during tensile deformation can be either a diffusion controlled or a plasticity-controlled process [13]. Diffusion of vacancies along the grain boundaries into cavities, which is an important mechanism in metals, plays little or no role in ceramics [1]. If cavities should grow by this diffusion mechanism then it is expected that the degree of cavitation would increase with decreasing strain rate, which is not observed. The lack of rounded or spherical cavities, as found by Langdon and co-workers, is according to these authors also a strong evidence for cavity growth by means of another process than diffusion. It is clear that a plasticity controlled cavity growth process takes place during biaxial tensile deformation of the ceramics studied. In this case cavity growth is dependent upon the level of applied stress and the growth rate of cavities increases with increasing strain rate and/or decreasing temperature, which is demonstrated in Fig. 5.

The degree of internal damage to the materials is generally measured in terms of cavity volume percent. The quantitative assessment of cavities near the fracture surface found that the cavity volume percent was 12.8%. Though

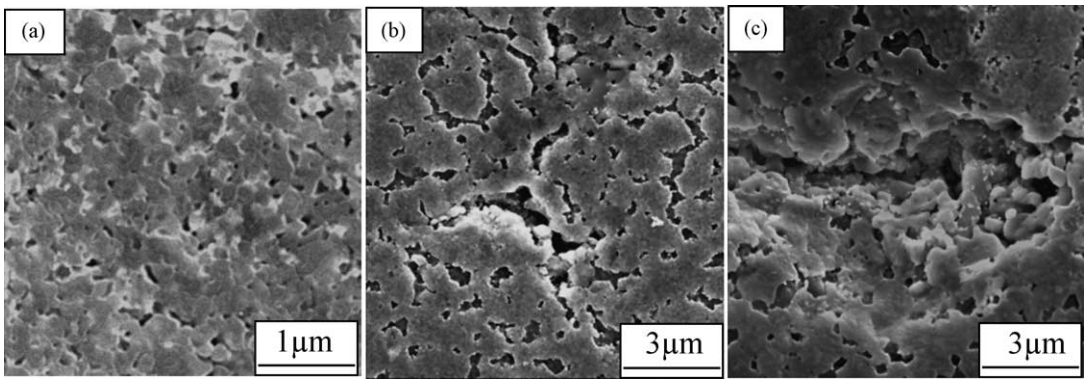

Fig. 6. Cavities morphology of the material in deep drawing at the punch rate of 0.6 mm·min^{-1} at 1400 °C with initial average grain size of 450 nm: (a) deep-drawn height of 4 mm, (b) deep-drawn height of 8 mm (c) deep-drawn height of 10.7 mm, fracture.

lots of internal cavities are prone to nucleate in Y–TZP and Al_2O_3–YTZ composites in uniaxial tensile tests, the cavity volume percent near the fracture surface reaches 30% [1]. The results prove that cavities cause premature failure at a relatively low volume percent under biaxial tensile stress, which means that the materials are very sensitive to the cavities and the cavities in multiaxial tensile stress state are more destructive than in uniaxial tension.

The sample with grain size of 230 nm can be deep drawn to the height of 12 mm at the punch rate of 0.6 mm·min^{-1}. The post-deformation structure of the sample showed that the cavities were mainly little crack-like voids and the cavity volume percent was only 3.1%. Considering that most shape forming processes require a tensile elongation around 100%, the internal damage found in this material is clearly within the range of practical use. These cavity damages are on par

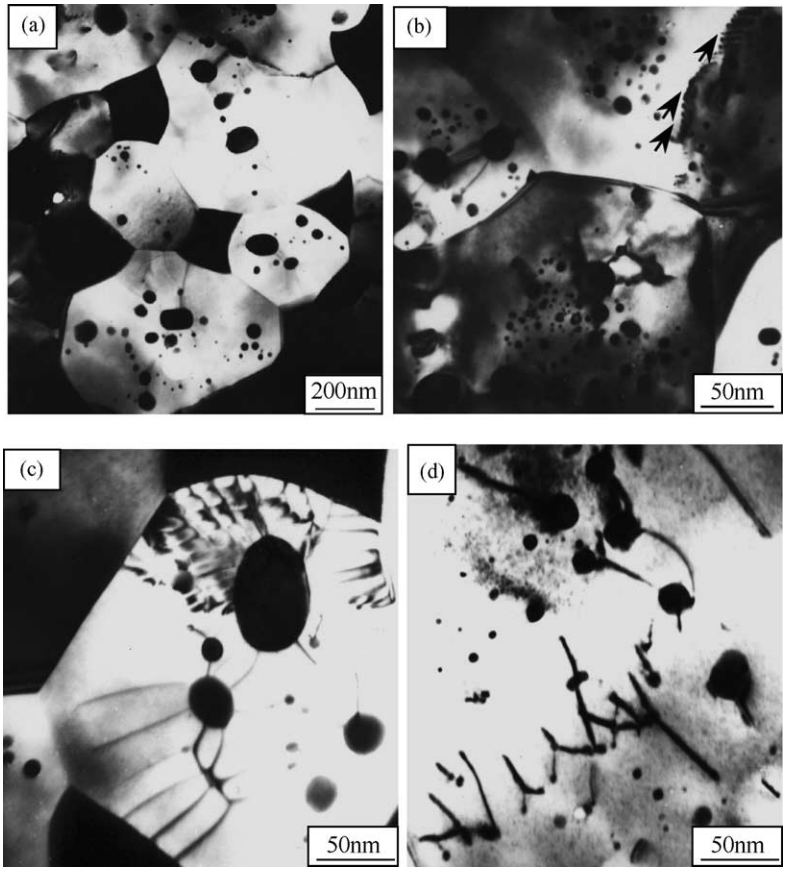

Fig. 7. TEM micrographs of (a) as-sintered and (b–d) deformed materials with initial average grain size of 230 nm. (a) As-sintered microstructure (the dark particles are zirconia grains and the large bright grains are alumina grains); (b) the post-deformation microstructure showing sub-boundaries inside the alumina grains indicating by the arrow; (c) and (d) showing the intragranular dislocation structure around nano-sized zirconia particles within alumina grains.

with those of currently used superplastic metals that have undergone tensile elongation.

One reason that this material was able to suppress cavity generation is that the zirconia grains scattered throughout the material underwent plastic deformation. This is unusual, because superplastic deformation usually occurs due to grain boundary sliding and makes almost no contribution to deformation within the grains. In fact, according to conventional wisdom, plastic deformation does not occur in superplastic ceramics in particular, because grain dislocations create a rigid body resistant to plastic deformation. Fig. 7 shows the deformed microstructure of the material with the initial grain size of 230 nm. There are multiple dislocations, dislocation networks and sub-boundaries inside the alumina grains. This kind of structure had not been seen before deformation, clearly demonstrating that it was generated during superplastic deep drawing and showing that active plastic deformation occurred within the grains through intragranular dislocation. Based on this, it is thought that in addition to diffusion, intragranular dislocation motion in alumina grains acted to mitigate localized stress concentrations and suppress cavity generation [14]. It is the first time that this phenomenon was observed in this kind of material in superplastic forming. Thus, the factors behind the above abnormal characteristics of the material are (1) the intragranular/intergranular nanocomposites of the material and the suppression of grain growth due to its two-phase composition, (2) lots of scattered intragranular nano-sized zirconia's particles brings out complex stress state in alumina grain, which makes it possible that the nucleation and movement of the dislocations in deformation and (3) the biaxial tension stress state in superplastic deep drawing.

It is proposed that this material can be thought of as a mixture of two grain sizes that respond to different deformation mechanisms: large alumina grains may deform by dislocation creep and small zirconia grains by grain boundary sliding, each being required to deform at the same strain rate. The overall behavior is governed by a combination of the behavior of the two grain sizes [15].

4. Conclusions

The main results obtained in this study are as follows:

(1) The heating of ethanol-aqueous salt solutions method of synthesis of powders is effective in reducing residual defects and increasing the homogeneity of particle dispersion. By using good dispersed nano-sized powders, intragranular/intergranular nanocomposites with the average grain size of 230 nm were obtained and the deformation behavior under biaxial stress by means of deep drawing was achieved.

(2) The cavities in ceramics are very sensitive to the grain size and also prone to cause premature failure at relatively lower cavity volume percent under biaxial tension stress state. The research also demonstrates that a plasticity controlled cavity growth process takes place in deformation.

(3) The intragranular dislocation structure and sub-boundaries around the nano-particles appears within alumina grains during biaxial deformation. This may be proved that intragranular dislocation creep is playing an important role in deformation.

Acknowledgements

This work was supported by the National Natural Science Foundation of China under grant number 50375037.

References

[1] T.G. Nieh, T. Wadsworth, O.D. Sherby, Superplasticity in Metals and Ceramics, Cambridge University Press, UK, 1997, pp. 105–116.
[2] B.N. Kim, K. Hiraga, Y. Sakka, B.K. Jang, Effect of cavitation on superplastic flow of 10% zirconia-dispersed alumina, Scripta Mater. 45 (2001) 61–67.
[3] S. Tekeli, High temperature ductility and cavitation behaviour of hot isostatically pressed (HIP) ZrO_2/Al_2O_3 composite containing 40 wt.% Al_2O_3, Ceram. Int. 29 (2003) 169–174.
[4] K. Hiraga, K. Nakano, T.S. Suzuki, Y. Sakka, Cavity formation and growth in a superplastic alumina containing zirconia particles, Mater. Sci. Forum 357–359 (2001) 193–198.
[5] K. Nakano, T.S. Suzuki, K. Hiraga, Y. Sakka, Superplastic tensile ductility enhanced by grain size refinement in a zirconia-dispersed alumina, Scripta Mater. 38 (1) (1998) 33–38.
[6] T.S. Suzuki, Y. Sakka, K. Morita, K. Hiraga, Enhanced superplasticity in an alumina-containing zirconia prepared by colloidal processing, Scripta Mater. 43 (2000) 705–710.
[7] B.N. Kim, K. Hiraga, K. Morita, Y. Sakka, Superplasticity in alumina enhanced by co-dispersion of 10% zirconia and 10% spinel particles, Acta Mater. 49 (2001) 887–895.
[8] W. Li, L. Gao, Nano ZrO_2 (Y_2O_3) particles processing by heating of ethanol-aqueous salt solutions, Ceram. Int. 27 (2001) 543–546.
[9] J.G. Li, T. Ikegami, J.H. Lee, T. Mori, Y. Yajima, Co-precipitation synthesis and sintering of yttrium aluminum garnet (YAG) powders: the effect of precipitant, J. Eur. Ceram. Soc. 20 (2000) 2395–2405.
[10] Y. Sakka, T.S. Suzuki, K. Morita, K. Nakano, K. Hiraga, Colloidal processing and superplastic properties of zirconia- and alumina-based nanocomposites, Scripta Mater. 44 (8) (2001) 2075–2078.
[11] A. Bataille, J. Crampon, R. Duclos, Upgrading superplastic deformation performance of fine-grained alumina by graphite particles, Ceram. Int. 25 (1999) 215–222.
[12] A.J.A. Winnubst, M.M.R. Boutz, Superplastic deep drawing of tetragonal zirconia ceramics at 1160 °C, J. Eur. Ceram. Soc. 18 (14) (1998) 2101–2106.
[13] Y. Ma, T.G. Langdon, A critical assessment of flow and cavity formation in a superplastic yttria-stabilized zirconia, Acta Metall. Mater. 42 (1994) 2753–2761.
[14] K. Morita, K. Hiraga, Reply to "Comment on the role of intragranular dislocations in superplastic yttria-stabilized zirconia", Scripta Mater. 48 (2003) 1403–1407.
[15] S. Tekeli, M. Erdogan, A quantitative assessment of cavities in 3 mol% yttria-stabilized tetragonal zirconia specimens containing various grain size, Ceram. Int. 28 (2002) 785–789.